

Uptake, effects, and regeneration of barley plants exposed to gold nanoparticles

Nadine S. Feichtmeier · Paul Walther · Kerstin Leopold

Received: 25 August 2014 / Accepted: 16 December 2014 / Published online: 6 January 2015
© Springer-Verlag Berlin Heidelberg 2015

Abstract Within the last years, nanogold has become more and more important in nanotechnology, for example, as catalyst or in medical applications. Its rising production, application, and disposal inevitably lead to an increased emission of gold nanoparticles (Au-NPs) in the environment. However, only little is known about the uptake and effects of Au-NPs on biota. The objective of this study was to investigate the reversibility and effects of citrate-coated Au-NP uptake into the model organism barley (*Hordeum vulgare* L.). For this purpose, barley seeds were cultivated in Au-NP-containing nutrient solution for 2 weeks before the seedlings were transferred into Au-NP-free media and grown for another 3 weeks. Stability of Au-NPs in the cultivation media was investigated over the 2-week exposure time. Gold content in the leaves and roots of the plants was measured after 2 weeks of exposure and after 7, 14, and 21 days of regeneration by means of total reflection X-ray fluorescence (TXRF) analysis after microwave-assisted digestion. Moreover, Au-NPs within plant material were localized by transmission electron microscopy (TEM) of ultrathin cross sections. The obtained results reveal that Au-NPs accumulate in the plant roots. Concentration-dependent effects on the uptake of macronutrients and micronutrients, as well as on biomass production of exposed plants, in particular, on root growth were observed. Even though

exposed barley plants were able to regenerate to a certain extent, their root growth was permanently decreased.

Keywords Au-NPs · Barley · Effects of nanogold · Regeneration · *Hordeum vulgare* L

Introduction

Nanomaterials are defined as solid materials with sizes between 1 and 100 nm in at least one dimension. This results in unique physicochemical properties that are not observed at the corresponding bulk material (Nel et al. 2006). Thus, they have received a lot of attention in industry and technology. In late 1996, the Nanotechnology Working Group in the USA estimated that the worldwide market for products with nanotechnology would reach \$1 trillion by 2015 (Roco 2005). Advances in synthesis and surface functionalization of nanoparticles have led to wide application of gold nanoparticles in many fields, such as industrial catalysis (Grisel et al. 2002), energy conversion (Ferry et al. 2010), or water purification (Ojea-Jiménez et al. 2012). In recent years, their use in biomedicine is growing rapidly due to their unique optical and photothermal properties, as well as their broad variety of easily accessible surface functionalization. Therefore, they have opened new opportunities in diagnostics and therapeutics (Giljohann et al. 2010). However, as a result of these unique physicochemical properties concern about potential adverse effects arise and their increasing production, use, and disposal will inevitably lead to their release into the environment. Modeled predicted environmental concentrations for gold nanoparticles are 0.14 $\mu\text{g L}^{-1}$ in natural waters and 5.99 $\mu\text{g kg}^{-1}$ in soils (Tiede et al. 2009). Consequently, studying the stability, mobility, bioavailability, and toxicity of

Responsible editor: Elena Maestri

Electronic supplementary material The online version of this article (doi:10.1007/s11356-014-4015-0) contains supplementary material, which is available to authorized users.

N. S. Feichtmeier · K. Leopold (✉)
Institute for Analytical and Bioanalytical Chemistry, University of
Ulm, Albert-Einstein-Allee 11, 89081 Ulm, Germany
e-mail: Kerstin.leopold@uni-ulm.de

P. Walther
Central Facility for Electron Microscopy, University of Ulm,
Albert-Einstein-Allee 11, 89081 Ulm, Germany

gold nanoparticles is important in order to assess potential risks for the environment, biota, and human health. In this context, the uptake and effects of gold nanoparticles (Au-NPs) on different biological systems have been studied. It is known yet that accumulation factors and toxicity of Au-NPs depend on particle size, shape, stability, surface functionality, and composition (Chithrani et al. 2006; Zhu et al. 2010).

No evidence of toxicity was observed in a study investigating the intraperitoneal administration of gold nanoparticles in mice in concentration ranges of 40, 200, and 400 $\mu\text{g kg}^{-1} \text{day}^{-1}$ (Lasagna-Reeves et al. 2010). In contrast to this, incubation with 13-nm citrate-capped gold nanoparticles causes a concentration-dependent reduction of cellular viability (Pernodet et al. 2006) as well as a significant reduction of life span and loss of weight of mice (Zhang et al. 2010). Judy et al. (2011) could demonstrate trophic transfer and biomagnification of nanogold from tobacco plants to tobacco hornworms by factors of up to 12 for treatments with 10-nm gold nanoparticles. However, most studies have so far been carried out with higher organisms, such as mice or fish. Research studies about interaction of gold nanoparticles with soil organisms (Judy et al. 2011, 2012; Sabo-Attwood et al. 2012) are very scarce and need to be examined further. Judy et al. (2012) demonstrated the bioavailability of gold nanomaterials to plants. After 7 days of exposure at 30 $\mu\text{g Au mL}^{-1}$ in the nutrient solution between 2 and 54 $\mu\text{g Au g}^{-1}$ were detected in the dried tobacco plant. Another study evaluated low or zero toxicity of gold, silver, and magnetite nanoparticles at doses of 62, 100, and 116 $\mu\text{g mL}^{-1}$ for cucumber and lettuce (Barrena et al. 2009). Investigations of Sabo-Attwood et al. (2012) suggest that gold nanoparticles enter tobacco plants through size-dependent mechanisms, translocate to cells, and cause toxic symptoms. The importance of plants, as base of the food chain, indicates further investigation of gold nanoparticle effects on plants. In particular, to our knowledge, no investigations have been carried out so far on the reversibility of uptake and effects of Au-NPs to barley plants. Such study could reflect batch emission scenario with temporarily high Au-NP exposure and fast decline to low or zero exposure and/or simulate effects of long-term accumulation of low exposure concentrations.

Hence, in the present study, barley plants were exposed to 10-nm citrate-coated gold nanoparticles at exposure concentrations ranging from 1 to 10 $\mu\text{g Au mL}^{-1}$ in order to investigate whether uptake and effects of the NPs is reversible. Au-NP stability in the exposure media, localization of Au-NPs in the plants, gold content in leaves and roots of the plants, and effects on barley plant growth over 2 weeks of exposure and 3 weeks of regeneration were studied.

Materials and methods

Preparation and characterization of gold nanoparticles

Citrate-stabilized Au-NPs were prepared according to Li and Leopold (2012) by chemical reduction of Au^{III} to Au^0 . For this purpose, 2 mL of a 1 % citric acid solution was added to 96 mL of ultrapure water (UPW) at room temperature (RT). After mixing, 1 mL of a 5-mM HAuCl_4 solution (Merck, Darmstadt, Germany) was added, giving a concentration of 0.05 mM HAuCl_4 in the mixture. One milliliter of a freshly prepared 1.98 M sodium borohydride (p.s.; Merck, Darmstadt, Germany) solution in 1 % citric acid (anhydrous, p.s.; Merck, Darmstadt, Germany) solution was added under vigorous stirring. The solution immediately became red indicating the formation of nanogold particles and was stirred for another 10 min. Size distribution of gold nanoparticle in this colloidal solution was investigated by transmission electron microscopy (TEM; ZEISS EM 10, Carl Zeiss Microscopy GmbH, Jena, Germany). Particle size of the formed spherical particles ranged from 2 to 21 nm (Fig. 1a). Finally, the gold

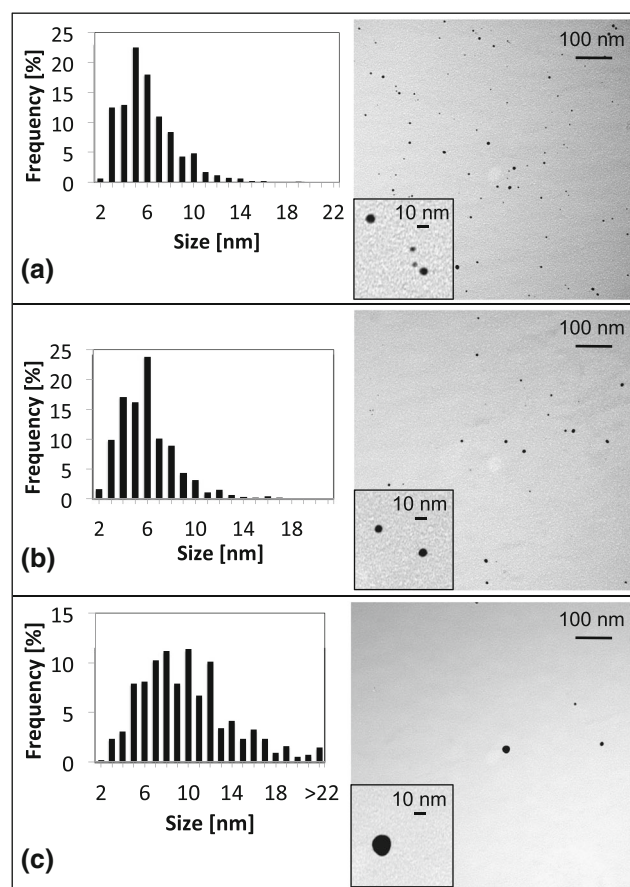


Fig. 1 Exemplary TEM images and histograms of corresponding particle size distribution of Au-NPs in (a) freshly synthesized Au-NP hydrosol, (b) nutrient medium at the start of the exposure experiment, and (c) nutrient medium after 2 weeks of exposure

concentration of the resulting Au-NP hydrosol that served as a stock solution was determined by total reflection X-ray fluorescence analysis (TXRF; S2 Picofox, Bruker, Berlin, Germany). The determination of the zeta potential of gold nanoparticles was carried out using Zetasizer Nano-ZS (Malvern Instruments Ltd., UK); the zeta potential is given as a mean of at least three replicate measurements. Due to the fact that the measurements were performed in aqueous solution, the Smoluchowski approximation was used to calculate the zeta potentials from the measured electrophoretic mobility. The UV-Vis spectra were recorded on a Specord S600 UV-Vis spectrophotometer (Analytik Jena, Jena, Germany) with 1-nm resolution and were also performed in three times per samples.

In order to check completeness of the reduction of Au^{III} to AuNPs, the gold nanoparticle hydrosol was dialyzed against citric acid and the Au concentration in the dialysate was measured by TXRF. For dialysis, a Nadir[®] membrane with an average pore size of 2.5 nm (Carl Roth GmbH & Co. KG, Karlsruhe, Germany) was swelled up for 30 min in UPW before 40 mL of the nanoparticle solution were injected. The membrane was then rinsed with UPW and immersed in 400 mL of 0.03 % citric acid for 17 h.

Transmission electron microscopy investigations

Colloidal gold particles were adsorbed on glow discharged carbon-coated copper grids and imaged in a ZEISS EM 10 transmission electron microscope (TEM; Carl Zeiss Microscopy GmbH, Jena, Germany) at an accelerating voltage of 80 kV. ImageJ software (National Institutes of Health, Bethesda, USA) served for measuring mean nanoparticle diameter; size distributions are based on counting at least 500 individual particles.

Germination and cultivation of barley plants

First, the barley (*Hordeum vulgare* L., cultivar Barke) seeds were pretreated under modified axenic conditions to ensure surface sterility. For this purpose, seeds were incubated for 1 min in ethanol (70 %, Merck, Darmstadt, Germany) and washed for 1 min with ultrapure water. Then, 5-min incubation in ethanol (70 %) was repeated twice, and finally, the caryopses were washed ten times with ultrapure water for 1 min, before they were allowed to swell up in ultrapure water for 24 h at room temperature in the dark. Then, barley was cultivated for 2 weeks in a hydroculture media according to a procedure first described by Battke et al. (2003). Briefly, ten barley seeds per batch were placed on a floating layer consisting of low-density polyethylene granulate (LD-PE). The granulate provides necessary anchorage of the plant roots and allows at the same time sufficient nutrient supply from the culture medium. Three identical batches were prepared in separate polypropylene (PP) beakers for each gold concentration (1, 3, 5, 8, and 10 $\mu\text{g mL}^{-1}$) and for the controls

(0 $\mu\text{g Au mL}^{-1}$). Nutrient solutions were prepared as follows: Adequate aliquots of the Au-NP hydrosol were diluted in UPW, and then, pH value was adjusted to 6.0–7.0 by addition of approximately 1 mL of a 2 mol L⁻¹ potassium hydroxide solution. Then, 0.022 g of a Murashige and Skoog basal medium (Sigma-Aldrich, St. Louis, USA) salt were added to serve as nutrients. For the control batches, a gold-free hydrosol was prepared by mixing adequate amounts of citric acid, sodium borohydride, hydrochloric acid, and potassium hydroxide in ultrapure water before the nutrient salt was added.

For germination, the beakers were covered with Parafilm (American Can Company, Greenwich, USA) and placed in a dark chamber at room temperature. After 2 days, the beakers were set in a controlled chamber with 16-h light and 8-h dark per day at a constant temperature of 21.5 °C. Barley plants were harvested after 14-day exposure by pulling the seedlings out of the PE-granulate and washing the roots by rinsing with UPW. For determination of fresh biomass, the leaves and roots were separated from the seeds. Leaf and root length was metered as the length between seed and tip of the leaf and the length between root tip and seed, respectively.

Regeneration experiments

For the regeneration study, nine identical batches of barley plants were cultivated and exposed for 14 days to either 0 (controls) or 5 $\mu\text{g mL}^{-1}$ Au-NP hydrosol according to the cultivation procedure described above. After 2 weeks, the seedlings were removed from the Au-NP-containing hydroculture media and their roots were rinsed with ultrapure water. Then, the barley plants were transferred into noncontaminated fresh media consisting of 0.022 g Murashige and Skoog basal medium in 100 mL ultrapure water and were allowed to grow for another 21 days in the controlled chamber with light/dark cycle and temperature set as given above. Barley plants from three identical beakers were harvested after 7, 14, or 21 days, respectively. Throughout the regeneration study, filling up to 100 mL with UPW kept the total volume of noncontaminated nutrient medium constant. Leaf and root lengths were documented, and gold concentrations in roots, leaves, and nutrient solution were checked by TXRF measurements.

Sample preparation for ultrathin cross sections

Root tips were fixed by immersion into 2.5 % of glutaraldehyde in phosphate buffer containing 1 % saccharose for 2 h at RT, followed by 1 % of osmium tetroxide for 2 h. Then, samples were dehydrated in a graded series of propanol and block contrasted with 2 % of uranyl acetate in ethanol and gradually embedded in Epon (Fluka Chemie AG, Buchs, Switzerland). Thin sections (thickness about 100 nm) were cut with an Ultramicrotome Ultracut (Leica Microsystems,

Wetzlar, Germany), equipped with a diamond knife (Diatome, Biel, Switzerland), and mounted on formvar-coated copper grids. The samples were imaged in a ZEISS EM 10 transmission electron microscope (TEM; Carl Zeiss Microscopy GmbH, Jena, Germany) at an accelerating voltage of 80 kV.

Sample preparation for TXRF measurement

The leaves and roots were dried at 120 °C for approx. 24 h until constant dry weight and then milled in an agate mortar. Complete decomposition of the material was achieved by microwave-assisted pressurized digestion in a MULTIWAVE (Anton Paar, Graz, Austria). For this purpose, the polytetrafluorometoxil liners were charged with up to 160 mg of dried and milled plant samples, 5 mL of nitric acid (HNO₃, 65 %, EMSURE® ISO, Merck) and 2 mL of hydrogen peroxide (H₂O₂, 31 %, VLSI Selectipur®, Merck). The digestion was performed at a maximum pressure of 60 bar and a maximum temperature of 260 °C applying 1000 W for 20 min. After cooling, the clear digests were transferred into 10-mL PE flasks and filled up to volume with UPW. These solutions were stored in a refrigerator at 4 °C until measurement.

Total reflection X-ray fluorescence measurement procedure for element quantification

The element contents of plants' digests, nutrient solution, and colloidal stock standard solution were determined by total reflection X-ray fluorescence (TXRF) analysis using S2 Picofox instrument (Bruker, Berlin, Germany) equipped with a molybdenum tube and silicon drift detector. The measurements were performed at a tube voltage of 50 kV, a current rating of 600 µA, and a lifetime of 1000 s. The selected lines and respective energies for quantification of Au, Ca, K, Mn, Fe, Zn, and for the internal standard V are given in Table 1. For internal calibration, an adequate volume of a vanadium (V) standard solution (NH₄VO₃ in 0.5 M HNO₃, 1000 mg V L⁻¹;

Table 1 Selected spectral lines and respective energies for K, Ca, V (internal standard), Mn, Fe, Zn, and Au for quantification by TXRF measurements

Element	Selected spectral line for quantification	Energy (keV)
K	Kα ₁	3.31
Ca	Kα ₁	3.69
V	Kα ₁	4.95
Mn	Kα ₁	5.90
Fe	Kα ₁	6.41
Zn	Kα ₁	8.64
Au	Lα ₁	9.71

Merck) was added to 1 mL of a sample solution. After thorough mixing, 10 µL of this solution were applied onto a quartz glass carrier, the liquid was evaporated, and the sample was measured by TXRF. The obtained values were corrected by the procedure blank. The detection limit (DL) for gold in the sample solution is 0.37 µg L⁻¹ corresponding to a method detection limit of 0.023 µg Au g⁻¹ in the dried biological material. Six replicates of each sample solution were measured.

Results and discussion

Characterization of gold nanoparticles and stability in the nutrient solution

In order to confirm complete transformation of ionic Au^{III} into zero-valent AuNPs, the resulting colloidal solution was dialyzed directly after synthesis. The Au concentration in the dialysate and in the colloidal AuNP solution was checked by TXRF measurements after 17 h. The data revealed that less than 1.82 % of the initial gold amount is transferred into the counter solution. Hence, complete reduction of Au^{III} and formation of AuNPs (larger than 2.5 nm) can be assumed.

The stabilization of gold nanoparticles by citric acid was investigated by zeta potential analysis. The zeta potential of the synthesized gold nanoparticles in the hydrosol was found to be -23.83 ± 2.31 mV at a pH of 2 to 3, proving the negatively charged surface of the particles due to the coating with citrate anions. These values were in good agreement with findings of Sun et al. (2009), reporting zeta potentials ranging from -1 to -30 mV depending on the pH value.

The elemental composition of the gold nanoparticle hydrosol was detected by TXRF (recorded spectrum, see Fig. S1). Beside the expected elements (Au from AuNPs and Cl from the precursor), the spectrum shows the presence of trace amounts of the abundant elements K, Ca, and Fe. However, these elements are in a negligible concentration (<0.5 mg L⁻¹) and much higher concentrations of these elements are added for preparation of the nutrient medium. In addition to size characterization by TEM after drying of AuNP hydrosol onto a grid, UV-Vis spectroscopy was employed to estimate the size of NPs directly in the hydrosol. Spectra were recorded from 300- to 900-nm wavelength to analyze the plasmon absorbance of the citrate-coated gold nanoparticle. The UV-Vis spectrum (Fig. S2) shows a maximum at $\lambda_{\max} = 518.5$ nm. For comparison, commercially available 20-nm-sized AuNPs were investigated showing surface plasmon resonance at $\lambda_{\max} = 523.5$ nm. Hence, the maximum absorbance of the synthesized AuNPs was in perfect agreement with the experimental data obtained from TEM investigation, revealing particle sizes from 2 to 19 nm (see Fig. 1a).

The stability of Au nanoparticles in the nutrient solutions was checked by TEM investigations at the start of the experiment and after 2 weeks in order to reveal any changes in the size of Au-NP. Images of Au-NPs in the nutrient media at the start of the experiment show individual spherical particles ranging in size from 2 to 19 nm (Fig. 1b). This is in good agreement with the characteristics of the synthesized Au-NPs in the original hydrosol used as stock solution (Fig. 1a). Hence, short-term stability of Au-NPs in the nutrient is thereby confirmed. However, as expected, after 2 weeks, TEM investigation illustrates some agglomeration of Au-NPs in the nutrient solution resulting in a broader size distribution (Fig. 1c).

Effects of gold nanoparticle exposure on barley plants

The exposure of barley seeds with Au-NPs up to a concentration of 10 µg mL⁻¹ in the nutrient medium showed no significant influence on seed germination (two sample *t* test, *p*=0.11; *P*=95 %). The average percentage of germination of all experiments was 86±9 %. However, a clear effect of exposure concentration on plant growth was observed (see Fig. 2). The leaves of exposed barley plants became yellow and necrotic whereas the roots colored dark brown. In addition, the produced fresh biomass per plant decreased with increasing exposure concentrations. Accordingly, the leaf and root lengths of the test species decreased with increasing Au-NP exposure concentration. The median leaf length of *Hordeum vulgare* L. after 2 weeks was 195 mm for controls and 41 mm for plants

exposed at the highest exposure concentration, respectively. However, a concentration of 1 µg mL⁻¹ of Au-NPs in the nutrient medium has a stimulating effect on the growth. It has been supposed that low doses of nanoparticles activate the repair mechanism of plants and so enhance their growth (hormesis effect) (Barrena et al. 2009). This increasing plant growth at low NP exposure concentrations and the decreasing plant growth at higher Au-NP concentrations is in good agreement with results reported by Racuciu and Creanga (2007), who investigated the effects of tetramethylammonium hydroxide (TMA-OH)-coated ferrophase particles on young popcorn plants.

The similar adverse effects on plant growth after exposure with metal nanoparticles were reported by Lin and Xing (2007) and Battke et al. (2008). These negative effects on plant growth and biomass production might be explained by adsorption of Au-NPs onto cell wall surfaces of the primary root diminishing the pore size and consequently inhibiting water transport capacity, which finally results in a reduced plant growth and weight. This effect was first described by Asli and Neumann (2009). In order to support this hypothesis, microscopic studies of the roots were performed in this work as described in the following.

Possible interactions of gold nanoparticles with plant roots are adsorption onto the surface, incorporation in the cell walls, and uptake into the cell (Nowack and Bucheli 2007). Hence, light microscopic and TEM investigations were performed in order to localize Au-NPs and effects in root tips (see Fig. 3). In light microscopy, the resolution of nanoparticles is not

Fig. 2 Concentration-dependent effects of Au-NP exposure on barley plants after 2 weeks of exposure. (a) Photos of barley seedlings, (b) fresh biomass of leaves (empty symbols) and roots (filled symbols) of barley plants (mean±one standard deviation for three individual batches with four to ten barley seedlings each), (c) leaf lengths, and (d) root lengths of barley plants (box plots represent median values including 14–21 individual data sets per concentration; bars give minimum and maximum value excluding outliers marked as red crosses)

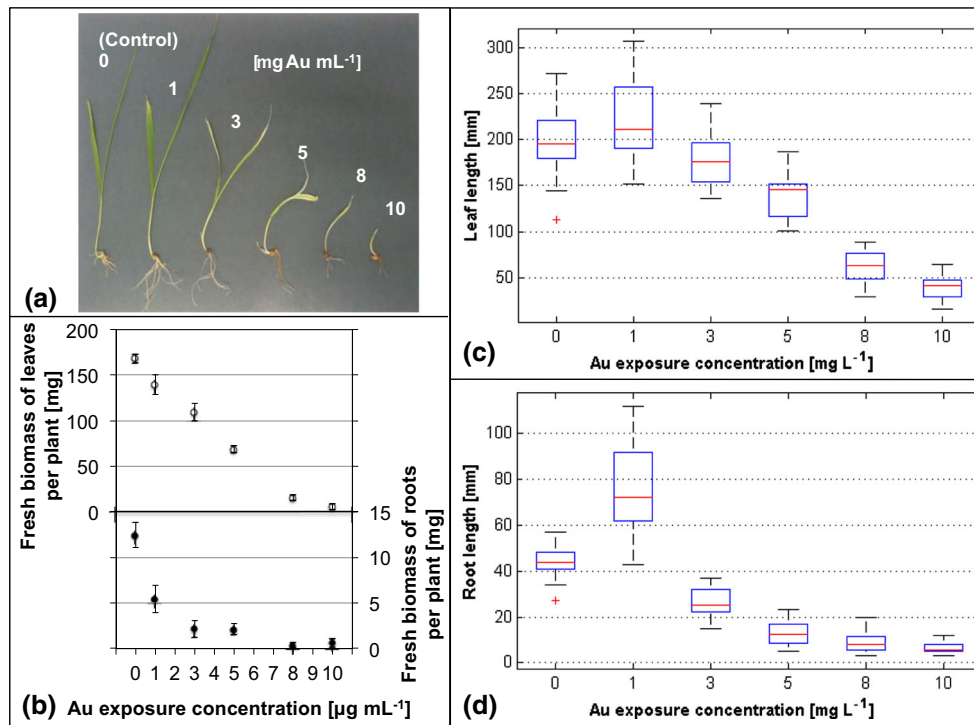
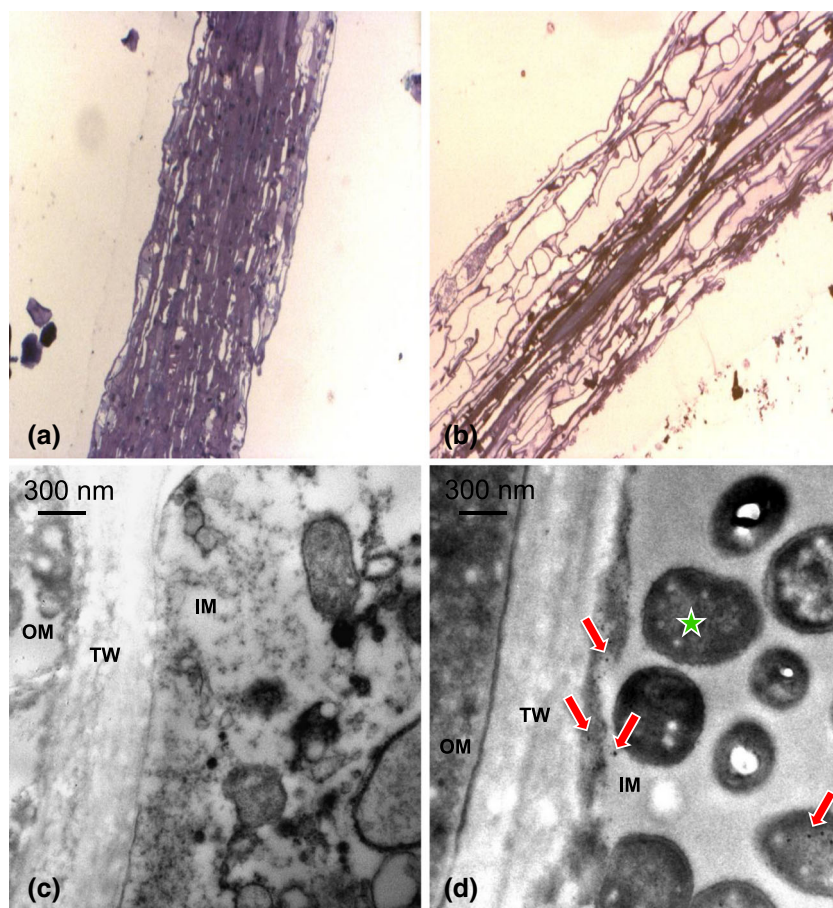


Fig. 3 Images of barley primary root tips. Light microscopic observation (magnification, ten times) of longitudinal sections of barley primary root tips of (a) control plants and (b) plants exposed to $10 \mu\text{g mL}^{-1}$ Au-NPs; TEM images of root cross sections of (c) control plants and (d) plants exposed to $10 \mu\text{g mL}^{-1}$ Au-NPs. Bacteria (*asterisk*) and gold nanoparticles (*arrows*). OM outer matrix, IM inner matrix, TW thick wall

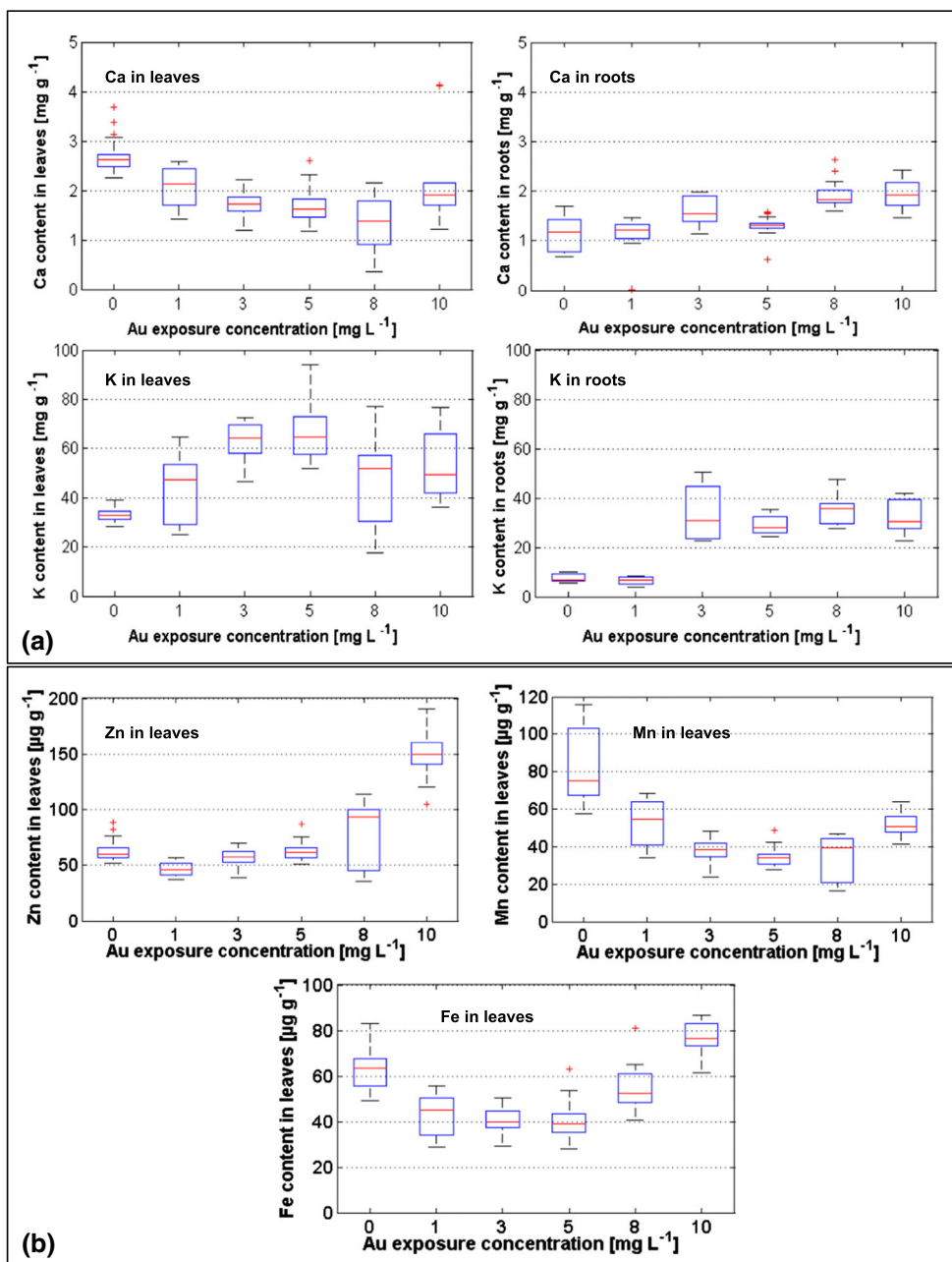


possible but visualization of probable effects is possible. Longitudinal sections of root tips clearly show differences in the morphology of the root tips of exposed plants to those of the control group. In contrast to the control sample in the exposed root, the epidermis is broken and the cortical cells are collapsed. TEM images of cross sections enable the visualization of the inner plant structure and may elucidate whether gold nanoparticles enter the plant's roots. Within exposed plant samples dark spots with a maximum size of 18 nm in diameter were observed, revealing the presence of (an) element(s) of higher atomic number than the surrounding. Even though a definite chemical characterization as Au-NP by energy dispersive X-ray spectrometry (EDX) was not possible due to the high dispersion of the NPs and the relatively low sensitivity of EDX in TEM, the absence of such spots in control plants as well as the appropriate size of the observed spots and the lack of any other possible explanation strongly suggest that the observed darker areas reflect the presence of Au-NPs. The nanoparticles are observed mainly inside the thick walls of exposed barley roots, suggesting an accumulation of the Au-NPs within the roots. This hypothesis is in good agreement with findings from Glenn et al. (2012) who observed 4-nm Au-NPs accumulated in root cells of freshwater aquatic plants and of Sabo-Attwood et al. (2012) who revealed

that gold nanoparticles could enter tobacco plants through the roots and are found in the vasculature and root cells.

In addition to the effects described above, possible changes in the elemental composition of the plant material were studied by TXRF analysis after decomposition of roots and leaves, respectively. In particular, the content of the macronutrients Ca and K (Fig. 4a) and the micronutrients Mn, Fe, and Zn (Fig. 4b) were evaluated, since they are classical markers of oxidative stress. The calcium concentration in leaves was not affected by exposure to AuNPs, since found values range all in a narrow range below 3 mg g^{-1} . These findings were in accordance with investigations of Biddulph et al. (1959), who found out that calcium is generally poorly translocated from roots to shoots. However, in roots exposed to AuNPs, slightly increasing Ca contents were observed, with median contents of 1.93 mg g^{-1} for treatments at 10 mg Au L^{-1} compared to 1.17 mg g^{-1} in control plants. The higher levels of calcium in exposed roots probably derive from a protection mechanism of the plant against the uptake of Au-NPs, since Ca is known to ameliorate toxicities and prevent leakage (True 1914). Observed effects of Au exposure to potassium concentrations were stronger and occurred in leaves as well as in roots. K levels in leaves increased from a minimum median value of 32.84 mg g^{-1} in control plants to 64.73 mg g^{-1} in plants

Fig. 4 Content of macronutrients (a) and micronutrients (b) in roots and leaves (dried material) of barley plants grown for 2 weeks in a nutrient solution spiked with Au-NPs (box plot represents median values including 18–27 individual data sets per concentration; bars give minimum and maximum value excluding outliers marked as red crosses)



exposed to 5 mg Au L⁻¹. The increasing influx of K might be explained by an increased permeability of the cell membrane for K⁺ ions (Foote and Hanson 1964). Exposure to 1 mg L⁻¹ Au-NPs did not impact potassium contents in plant roots. However, higher levels of Au treatment led to significantly higher K concentrations in roots of up to 35.92 mg g⁻¹, with similar values regardless Au exposure concentrations.

Regarding the micronutrients, their content in the roots varies in a broad range for the controls and therefore no significant changes could be observed for the exposed plants (see supplementary information, Fig. S3). For the leaves, the observed concentration ranges are narrower and allow interpretation of

the obtained data (Fig. 4b). Manganese levels slightly decreased with increasing Au concentration in nutrient medium from median 74.99 μg g⁻¹ in control plants to 33.86 μg g⁻¹ in plants treated with 5 mg L⁻¹ Au-NPs. Zn contents in exposed plant leaves, in contrast, increased from 60.39 μg g⁻¹ in the controls up to 149.46 μg g⁻¹ in leaves of plants exposed to 10 mg L⁻¹ Au-NPs. For iron contents in plant leaves, a minimum content of 39.80 μg g⁻¹ was found for an exposure concentration of 3 mg Au L⁻¹, and the highest value of 86.53 μg Fe g⁻¹ was found in leaves exposed to 10 mg Au L⁻¹.

In summary, the exposure of plants to citrate-stabilized gold nanoparticles results in more or less increasing contents

of Ca, K, Zn, and Fe and decreasing concentration of Mn. Hence, the observed adverse effects on plant growth after exposure to citrate-stabilized gold nanoparticles do not derive from nutrient deficiency.

Gold nanoparticle uptake

In addition to observation of effects, the uptake of the gold nanoparticles was quantified by measurement of the total amount of gold taken-up into roots and leaves of the seedlings within the 2 weeks of exposed growth (see Fig. 5a). The gold content in barley roots rises with increasing gold concentration in the nutrient medium from below the detection limit of $0.023 \mu\text{g g}^{-1}$ in control plants to a maximum of $623 \mu\text{g g}^{-1}$ in plants exposed at $8 \mu\text{g Au mL}^{-1}$. At the highest initial exposure concentration of $10 \mu\text{g Au mL}^{-1}$, slightly lower values occurred. An explanation for this might be that more aggregated particles are formed and settle down leading to a lower actual concentration of gold nanoparticles available for plant uptake. Moreover, the distribution of data became generally broader at higher exposure concentrations, which might be explained by the presence of NPs agglomerates that are attached to the surface of the roots.

In the leaves, however, gold concentration was below $0.023 \mu\text{g g}^{-1}$ for all investigated plants, except for one out of three batches exposed to $10 \mu\text{g mL}^{-1}$, where a value of $3.84 \mu\text{g g}^{-1}$, was observed. Since all other values were below detection limit, it was regarded as an outlier caused most probably by contamination. Hence, no significant transport of gold nanoparticles from the roots into the shoots occurred within the 2-week exposure period. This is in agreement with findings reported by Judy et al. (2012) who exposed tobacco plants to 10-, 30-, and 50-nm Au-NPs for 4 weeks. In previous studies, our group investigated the uptake of palladium nanoparticles (Pd-NPs; size 5–10 nm) in barley plants applying identical exposure conditions (Battke et al. 2008; Leopold and Schuster 2011). Comparing the uptake of Au- and Pd-NPs

into the barley plants and their effects on plant growth, the following differences were observed: Pd concentrations found in roots of barley plants were higher than Au concentrations, ranging from 214 to $987 \mu\text{g g}^{-1}$ of the dried material at exposure concentrations ranging from 1.1 to $10.6 \mu\text{g mL}^{-1}$. Moreover, transport of Pd-NPs from the roots into the leaves was observed, resulting in Pd contents in the dried leaves that increased from 0.029 to $0.879 \mu\text{g g}^{-1}$ with rising exposure concentration. However, the observed adverse effects on the plant growth were similar for both metal NPs.

Regeneration and release of Au-NPs

Finally, investigations have been carried out on the reversibility of uptake and effects of Au-NPs to barley. Taking into account that Au-NPs mainly accumulate at and in the roots, it seems probable that at some extent, Au-NPs may be released back into the nutrient solutions when exposure concentrations diminish. Hence, barley seedlings first exposed to $5 \mu\text{g mL}^{-1}$ Au-NPs for 14 days were then transferred into Au-free nutrient media and grown for another 21 days. During regeneration experiment, Au concentration in the nutrient solution was investigated. For this purpose, three samples were taken from each of the three batches and measured in triplicate. Most replicates were below the detection limit of $0.37 \mu\text{g Au L}^{-1}$. However, after 7 days in two samples, Au concentrations above the detection limit were found and could be quantified, after 14 days in nine samples, and after 21 days in five samples, suggesting the release of Au-NPs from the barley seedling into the solution (see Table 2). Hence, gold content in barley leaves and roots was checked after 0, 7, 14, and 21 days of regeneration (Fig. 5b). A decrease in Au contents in the roots is obvious already after 7 days of regeneration in Au-free media. However, after 14 and 21 days, no further decline was observed. Hence, it seems probable that only Au-NPs adsorbed to the surface of the roots are released, whereas those that had entered the plants remained within.

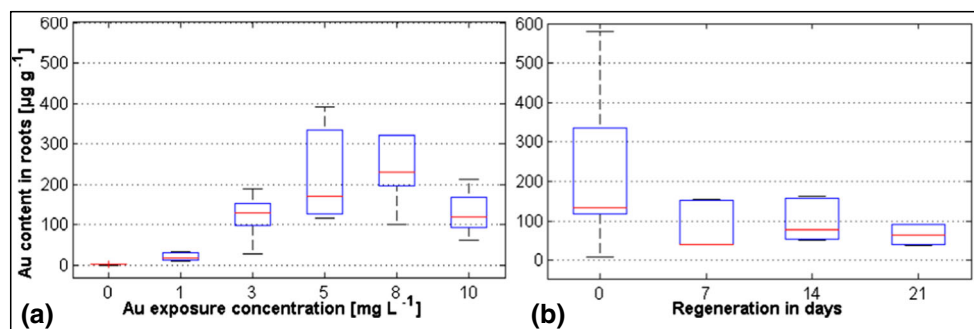


Fig. 5 Au content in roots (in $\mu\text{g g}^{-1}$ dried material) of barley plants: (a) grown for 2 weeks in a nutrient solution spiked with Au-NPs (box plot represents median, minimum, and maximum values including 9–18 individual data sets per concentration) and (b) after 0, 7, 14, and 21 days

of regeneration of barley plants exposed for 2 weeks at $5 \mu\text{g Au mL}^{-1}$ (box plot represents median values including 9–18 individual data sets per regeneration period; bars give minimum and maximum values)

Table 2 Mean gold concentration in nutrient solution during regeneration experiment and number of values above detection limit (DL)

Regeneration in days	Mean Au concentration ($\mu\text{g mL}^{-1}$)	Number of values above DL
0	<0.37	0
7	1.50±0.71	2
14	2.63±1.22	9
21	2.40±1.34	5

Nevertheless, no gold was detected in the leaves (detection limit $0.023 \mu\text{g g}^{-1}$) during regeneration experiment for all batches. Hence, a transport of gold nanoparticles from the roots into the shoots even after 2-week exposure and 3-week regeneration time was not observed even though Au content in the roots remained significant. Moreover, the replanting of barley seedlings into noncontaminated nutrient media led to an approximation of leaf length of initially exposed plants and control plants giving no significant differences after 7 days of regeneration (Fig. 6a), whereas the differences in root length

between control and exposed plants became more significant ($p=0.02$; $P=95\%$) over time, i.e., initially exposed plants have reduced root growth (Fig. 6b). These observations suggest that the observed destruction of root epidermis and the collapse of cortical cells are irreversible.

Conclusions

The present study demonstrates the concentration-dependent uptake and effects of citrate-coated 10-nm Au-NPs in barley. Seed germination was not affected by gold nanoparticles within an exposure concentration range from 1 to $10 \mu\text{g Au mL}^{-1}$, whereas plant growth was strongly affected, resulting primarily in significantly lower production of biomass at exposure concentrations equal and higher than $3 \mu\text{g Au mL}^{-1}$. Taking into account the modeled predicted environmental concentrations of Au-NPs in the environment (Tiede et al. 2009) of maximum $0.006 \mu\text{g g}^{-1}$ in soils, it can be speculated that no significant adverse effects on the test species barley will occur after short-term exposure. However, further studies should be carried out in order to assess phytotoxicity of Au-NPs at low-level long-term exposure, since accumulation of Au-NPs in the roots was found to be irreversible. Moreover, the regeneration experiments revealed that short-term exposure to high concentrations of Au-NPs causes permanent damage of the plant’s roots. TEM images of root tip cross sections disclosed accumulation and internalization of Au-NPs in the roots. Nevertheless, uptake of gold nanoparticles was only observed in plant roots and no transfer into the leaves occurred within 2 weeks of exposure and 3 weeks of regeneration. This finding differs from the results found in analogous exposure studies with Pd-NPs of similar size, where Pd was also found in the leaves of exposed barley plants (Leopold and Schuster 2011). Hence, translocation mechanism of NPs within barley plants is apparently also controlled by the chemical nature of the nanoparticle itself and not only by the size of the particles.

Acknowledgments The authors would like to thank Josef Breun GmbH & Co. KG for providing barley seeds. We also acknowledge R. Schindl and K. Wörle (Institute for Analytical and Bioanalytical Chemistry, University of Ulm) for assistance with TEM measurements.

Author contributions The manuscript was written through contributions of all authors. All authors have given approval to the final version of the manuscript.

Conflict of interest The authors declare no conflict of interest.

References

Asli S, Neumann PM (2009) Colloidal suspensions of clay or titanium dioxide nanoparticles can inhibit leaf growth and transpiration via physical effects on root water transport. *Plant Cell Environ* 32(5): 577–584

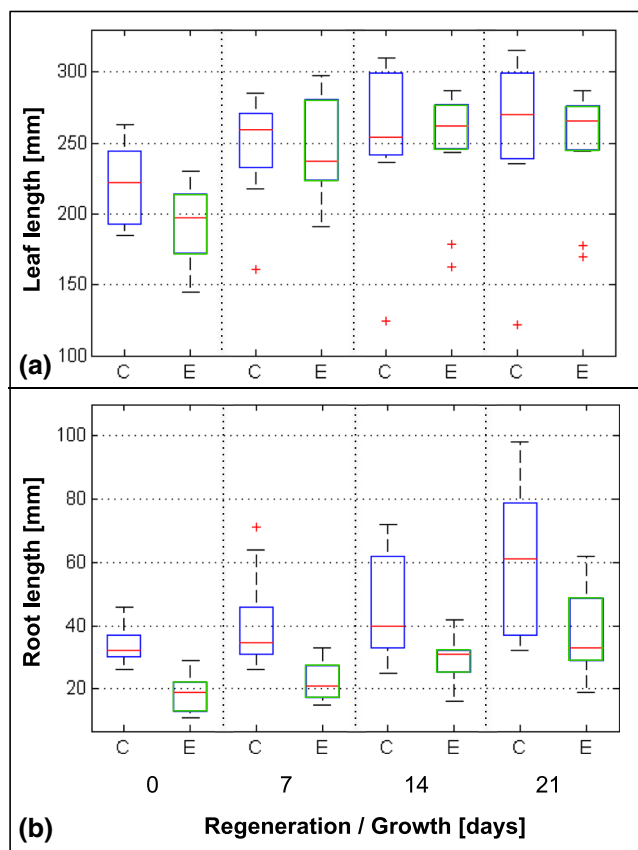


Fig. 6 Time-dependent regeneration after Au-NP exposure and 0, 7, 14, and 21 days of growth in Au-free medium: (a) leaf lengths and (b) root lengths of barley plants initially exposed to $5 \mu\text{g Au mL}^{-1}$ (“E”, green boxes) and nonexposed controls (“C”, blue boxes) (box plot represents median values including 9–14 individual data sets per regeneration period; bars give minimum and maximum values excluding outliers marked as red crosses)

- Barrena R, Casals E, Colón J, Font X, Sánchez A, Puentes V (2009) Evaluation of the ecotoxicity of model nanoparticles. *Chemosphere* 75(7):850–857
- Battke F, Schramel P, Ernst D (2003) A novel method for in vitro culture of plants: cultivation of barley in a floating hydroponic system. *Plant Mol Biol Report* 21(4):405–409
- Battke F, Leopold K, Maier M, Schmidhalter U, Schuster M (2008) Palladium exposure of barley: uptake and effects. *Plant Biol* 10(2):272–276
- Biddulph O, Cory R, Biddulph S (1959) Translocation of calcium in the bean plant. *Plant Physiol* 34:512–519
- Chithrani BD, Ghazani AA, Chan WCW (2006) Determining the size and shape dependence of gold nanoparticle uptake into mammalian cells. *Nano Lett* 6(4):662–668
- Ferry VE, Munday JN, Atwater HA (2010) Design considerations for plasmonic photovoltaics. *Adv Mater* 22(43):4794–4808
- Footo BD, Hanson JB (1964) Ion uptake by soyabean root tissue depleted of calcium by EDTA. *Plant Physiol* 39:450–460
- Giljohann DA, Seferos DS, Daniel WL, Massich MD, Patel PC, Mirkin CA (2010) Gold nanoparticles for biology and medicine. *Angew Chem Int Ed* 49(19):3280–3294
- Glenn JB, White SA, Klaine SJ (2012) Interactions of gold nanoparticles with freshwater aquatic macrophytes are size and species dependent. *Environ Toxicol Chem* 31(1):194–201
- Grisel R, Weststrate K-J, Gluhoi A, Nieuwenhuys BE (2002) Catalysis by gold nanoparticles. *Gold Bull* 35(2):39–45
- Judy JD, Unrine JM, Bertsch PM (2011) Evidence for biomagnification of gold nanoparticles within a terrestrial food chain. *Environ Sci Technol* 45(2):776–781
- Judy JD, Unrine JM, Rao W, Wirick S, Bertsch PM (2012) Bioavailability of gold nanomaterials to plants: importance of particle size and surface coating. *Environ Sci Technol* 46(15):8467–8474
- Lasagna-Reeves C, Gonzalez-Romero D, Barria MA, Olmedo I, Clos A, Sadagopa Ramanujam VM, Urayama A, Vergara L, Kogan MJ, Soto C (2010) Bioaccumulation and toxicity of gold nanoparticles after repeated administration in mice. *Biochem Biophys Res Commun* 393(4):649–655
- Leopold K, Schuster M (2011) Pd particles as standardized test material for bioavailability studies of traffic related Pd emissions to barley plants. In: Zereini F, Wiseman CLS (eds) *Urban airborne particulate matter*. Springer Berlin Heidelberg, Heidelberg, pp 399–410
- Li L, Leopold K (2012) Ligand-assisted extraction for separation and preconcentration of gold nanoparticles from waters. *Anal Chem* 84(9):4340–4349
- Lin D, Xing B (2007) Phytotoxicity of nanoparticles: inhibition of seed germination and root growth. *Environ Pollut* 150(2):243–250
- Nel A, Xia T, Mädler L, Li N (2006) Toxic potential of materials at the nanolevel. *Science* 311(5761):622–627
- Nowack B, Bucheli TD (2007) Occurrence, behavior and effects of nanoparticles in the environment. *Environ Pollut* 150(1):5–22
- Ojea-Jiménez I, López X, Arbiol J, Puentes V (2012) Citrate-coated gold nanoparticles as smart scavengers for mercury(II) removal from polluted waters. *ACS Nano* 6(3):2253–2260
- Pernodet N, Fang X, Sun Y, Bakhtina A, Ramakrishnan A, Sokolov J, Ulman A, Rafailovich M (2006) Adverse effects of citrate/gold nanoparticles on human dermal fibroblasts. *Small* 2(6):766–773
- Racuciu M, Creanga D-E (2007) TMA-OH coated magnetic nanoparticles internalized in vegetal tissue. *Rom J Physiol* 52(3–4):395–402
- Roco MC (2005) Environmentally responsible development of nanotechnology. *Environ Sci Technol* 39(5):106A–112A
- Sabo-Attwood T, Unrine JM, Stone JW, Murphy CJ, Ghoshroy S, Blom D, Bertsch PM, Newman L (2012) Uptake, distribution and toxicity of gold nanoparticles in tobacco (*Nicotiana xanthi*) seedlings. *Nanotoxicology* 6(4):353–360
- Sun L, Zhang Z, Wang S, Zhang J, Li H, Ren L, Weng J, Zhang Q (2009) Effect of pH on the interaction of gold nanoparticles with DNA and application in the detection of human p53 gene mutation. *Nanoscale Res Lett* 4:216–220
- Tiede K, Hasseløev M, Breitbarth E, Chaudhry Q, Boxall ABA (2009) Considerations for environmental fate and ecotoxicity testing to support environmental risk assessments for engineered nanoparticles. *J Chromatogr A* 1216:503–509
- True RH (1914) The harmful action of distilled water. *Am J Bot* 1:255–273
- Zhang X-D, Wu H-Y, Wu D, Wang Y-Y, Chang J-H, Zhai Z-B, Meng A-M, Liu P-X, Zhang L-A, Fan F-Y (2010) Toxicologic effects of gold nanoparticles in vivo by different administration routes. *Int J Nanomedicine* 5:771–781
- Zhu Z-J, Carboni R, Quercio MJ, Yan B, Miranda OR, Anderton DL, Arcaro KF, Rotello VM, Vachet RW (2010) Surface properties dictate uptake, distribution, excretion, and toxicity of nanoparticles in fish. *Small* 6(20):2261–2265